

Resonant Spin Excitation in an Overdoped High Temperature Superconductor

H. He¹, Y. Sidis², P. Bourges², G.D. Gu³, A. Ivanov⁴, N. Koshizuka⁵, B. Liang¹,
C.T. Lin¹, L. P. Regnault⁶, E. Schoenher¹, and B. Keimer^{1,7}

¹*Max-Planck-Institut für Festkörperforschung, 70569 Stuttgart, Germany.*

²*Laboratoire Léon Brillouin, CEA-CNRS, CE-Saclay, 91191 Gif sur Yvette, France.*

³*Department of Advanced Electronic Materials, School of Physics, University of New South Wales, Sydney 2052, Australia.*

⁴*Institut Laue Langevin, 156X, 38042 Grenoble cedex 9, France.*

⁵*SRL/ISTEC, 10-13, Shinonome 1-chome, Koto-ku, Tokyo 135, Japan.*

⁶*CEA Grenoble, Département de Recherche Fondamentale sur la Matière Condensée, 38054 Grenoble cedex 9, France.*

⁷*Department of Physics, Princeton University, Princeton, NJ 08544*

(November 23, 2018)

An inelastic neutron scattering study of overdoped $\text{Bi}_2\text{Sr}_2\text{CaCu}_2\text{O}_{8+\delta}$ ($T_c = 83$ K) has revealed a resonant spin excitation in the superconducting state. The mode energy is $E_{\text{res}} = 38.0$ meV, significantly lower than in optimally doped $\text{Bi}_2\text{Sr}_2\text{CaCu}_2\text{O}_{8+\delta}$ ($T_c = 91$ K, $E_{\text{res}} = 42.4$ meV). This observation, which indicates a constant ratio $E_{\text{res}}/k_B T_c \sim 5.4$, helps resolve a long-standing controversy about the origin of the resonant spin excitation in high-temperature superconductors.

A resonant spin excitation [1–8] with wave vector (π, π) has recently emerged as a key factor in the phenomenology of the copper oxide superconductors. In particular, prominent features in angle-resolved photoemission [9–11] and optical conductivity [12,13] spectra have been attributed to interactions of this bosonic mode with fermionic quasiparticles. The implications of these observations for the mechanism of high temperature superconductivity are under intense scrutiny, especially following suggestions that the spectral weight of the mode (which, at least in optimally doped $\text{YBa}_2\text{Cu}_3\text{O}_{6+x}$, is present only below the superconducting transition temperature, T_c [3,4]) provides a measure of the condensation energy [14,15] or condensate fraction [16] of the superconducting state. Several fundamentally different microscopic descriptions of the neutron data have been proposed. Some of these [3,17] attribute the resonance peak to the threshold of the particle-hole (ph) spin-flip continuum at $\lesssim 2\Delta_{\text{SC}}$ where Δ_{SC} is the energy gap in the superconducting state, others [11,18,19] to a magnon-like collective mode whose energy is bounded by the gap. Although the starting points of these calculations are disparate (itinerant band electrons in [11,17,18], localized electrons in [19]), the excitations corresponding to the neutron peak are described by the same quantum numbers (spin 1 and charge 0). In a completely different approach [20], the neutron data are interpreted in terms of a collective mode in the particle-particle (pp) channel whose quantum numbers are spin 1 and charge 2. The pp continuum that provides the upper bound for the pp resonance in the latter model is unaffected by superconductivity. Despite the central significance of this issue, there is still no “smoking gun” experiment selecting the correct theoretical approach.

A careful measurement of the doping dependence of the mode energy, E_{res} , can help resolve this issue. In Refs. [18–20], the mode is interpreted as a soft mode

whose energy is expected to decrease as a magnetic instability is approached with decreasing hole content. This is made explicit in an expression derived from the pp model which predicts that E_{res} is proportional to the doping level [20]. The behavior observed in underdoped $\text{YBa}_2\text{Cu}_3\text{O}_{6+x}$ [5–7] is consistent with that prediction. This alone, however, does not amount to a “smoking gun” because it can also be understood in the framework of the simple ph pair production model where $E_{\text{res}} \propto T_c$. In underdoped samples, T_c in turn is monotonically related to the hole content. Further difficulties derive from ambiguities associated with the distinction between the normal-state “pseudo-gap” in the charge sector and the true superconducting gap in the underdoped state. These are mirrored in the spin sector by uncertainties regarding the relationship between a broad peak observed by neutron scattering in the normal state [5–7] and the sharp resonant peak in the superconducting state.

The neutron data on underdoped samples therefore do not discriminate clearly between the very different theories of the resonance peak. Here we report a neutron scattering study in the overdoped state of $\text{Bi}_2\text{Sr}_2\text{CaCu}_2\text{O}_{8+\delta}$ where none of these complicating factors are present. In particular, T_c is reduced while the hole content keeps increasing, and the normal-state pseudogap disappears.

To this end, we used an array comprising eight small (individual volumes ~ 0.03 cm³), high quality overdoped $\text{Bi}_2\text{Sr}_2\text{CaCu}_2\text{O}_{8+\delta}$ single crystals grown by the floating-zone method [21]. In their as-grown state, the crystals were optimally doped, with $T_c \sim 91$ K, as was the sample used for our previous neutron study [8]. Using established procedures [22], they were subsequently annealed at 650°C under oxygen flow for 200 hours. (The long annealing time was used as a precaution. Previous studies [22] have shown that 20 hours are sufficient to achieve a homogeneous oxygen content for identically prepared samples.) Following this, the individual samples exhib-

ited sharp (width 5-7 K) superconducting transitions at 83 K, in excellent agreement with prior results [22]. Representative data measured by SQUID magnetometry are shown in the inset to Fig. 4. The crystals were co-aligned by x-ray Laue diffraction and mounted in an aluminum holder. The overall mosaicity of the array, $\sim 5^\circ$, was comparable to the angular dependence of the magnetic signal of the previous study [8] and therefore of little consequence for the signal intensity. However, compared to our previous experiment on a monolithic, optimally doped single crystal, the imperfect alignment of the crystal array would introduce additional uncertainties into an absolute intensity unit calibration which will therefore not be given here. In order to establish an optimal basis for a comparison of the results on optimally doped and overdoped samples, the experimental setup precisely duplicated the one used for the previous study [8]. The experiments were conducted on the triple axis spectrometer IN8 (at the Institut Laue-Langevin in Grenoble, France) in a focusing configuration with Cu(111) monochromator, pyrolytic graphite (002) analyzer, and 35 meV fixed final energy. The wave vector $Q = (H, K, L)$ is given in reciprocal lattice units (r.l.u.), that is, in units of the reciprocal lattice vectors $a^* \sim b^* \sim 1.64 \text{ \AA}^{-1}$ and $c^* \sim 0.20 \text{ \AA}^{-1}$. In these units, the in-plane wave vector (π, π) is equivalent to $(\frac{h}{2}, \frac{k}{2})$ with h, k odd integers. The data were taken with L set close to the maximum of the intensity modulation due to magnetic coupling of the bilayers ($L = -13.2$ or $L = -14$ for $\text{Bi}_2\text{Sr}_2\text{CaCu}_2\text{O}_{8+\delta}$ [8]).

$\text{Bi}_2\text{Sr}_2\text{CaCu}_2\text{O}_{8+\delta}$ is a highly complex material with a multitude of densely spaced phonon branches, not to mention the additional lattice dynamical complexity due to the incommensurate modulation of the Bi-O layer. Raw neutron data therefore show a large, featureless background predominantly due to unresolved single-phonon events. An example is given in Fig. 1. Building on lessons drawn from work on $\text{YBa}_2\text{Cu}_3\text{O}_{6+x}$, we have previously established [8] how the magnetic signal can be separated from this background by virtue of its characteristic energy, momentum, and temperature dependences. Specifically, the magnetic resonance peak that is the primary focus of the present study gives rise to a magnetic signal at wave vector $Q = (\pi, \pi)$ that shows a sharp upturn below T_c (Refs. [3-6,8]). The first step therefore involves taking the difference between the measured spectra in the superconducting and normal states and studying the energy and wave vector dependence of the enhanced signal. Figs. 2 and 3 show that this is confined to a narrow region in energy and wave vector centered at $E = 38 \text{ meV}$ and $Q = (\pi, \pi)$, while the background away from this region is reduced upon cooling. (The temperature dependence of the background becomes more pronounced at low energies, because the phonon scattering follows the Bose population factor $(1 - \exp(-E/k_B T))^{-1}$.) This is precisely the signature of the magnetic resonance peak observed in $\text{YBa}_2\text{Cu}_3\text{O}_{6+x}$

and optimally doped $\text{Bi}_2\text{Sr}_2\text{CaCu}_2\text{O}_{8+\delta}$.

The data on overdoped and optimally doped $\text{Bi}_2\text{Sr}_2\text{CaCu}_2\text{O}_{8+\delta}$ (also shown for comparison in Fig. 2) were fitted to a Gaussian magnetic resonant mode on top of a phonon background whose energy dependence is determined independently from scans at high temperatures and from constant- q scans away from (π, π) . The phonon background is multiplied by the Bose population factor, and the difference between the Bose factors at low and high temperatures gives rise to the negative signal at low energies in the difference plots. (The fact that the high temperature scan was taken at 100 K for the material with $T_c = 91 \text{ K}$, and at 90 K for the one with $T_c = 83 \text{ K}$, was taken into account in this analysis and did not influence the result.) Apart from an overall scale factor, there are two free parameters in the fit: The intensity of the resonant mode with respect to the phonon background, and its position. The results of these fits are shown in Fig. 2. The resonance energies extracted in this manner for optimally doped and overdoped $\text{Bi}_2\text{Sr}_2\text{CaCu}_2\text{O}_{8+\delta}$ are $42.4 \pm 0.8 \text{ meV}$ and $38.0 \pm 0.6 \text{ meV}$, respectively (95% confidence limits). If the assumption of equal widths of the resonant mode in both samples is relaxed, the relative position extracted from the fits is hardly affected. Likewise, a Lorentzian profile for the resonant mode also gave the same result within the error. The null hypothesis (no energy shift) can therefore be ruled out with a statistical confidence well exceeding 95%.

Before discussing the implications of these data, we proceed to the second step in the identification of the resonance peak, namely, the determination of the onset temperature of the magnetic signal. The temperature dependence of the peak magnetic intensity, shown in Fig. 4, indeed exhibits the strong upturn around $T_c = 83 \text{ K}$ that characterizes the resonance peak. Interestingly, this upturn is even sharper here than in the optimally doped sample. As in optimally doped $\text{YBa}_2\text{Cu}_3\text{O}_7$ (Refs. [3,4]) and $\text{Bi}_2\text{Sr}_2\text{CaCu}_2\text{O}_{8+\delta}$ (Ref. [8]), there is no evidence of magnetic scattering above T_c although this determination is limited by the high nuclear background.

The data shown in Figs. 2-4 are an essential complement to an extensive data set on the resonance peak in underdoped $\text{YBa}_2\text{Cu}_3\text{O}_{6+x}$. (Note that some [5], but not all [3], data on the resonant mode in slightly overdoped $\text{YBa}_2\text{Cu}_3\text{O}_7$ also exhibit a subtle trend towards lower energies. However, the data of Ref. [5] were taken under conditions different from those on underdoped and optimally doped $\text{YBa}_2\text{Cu}_3\text{O}_{6+x}$, which prevents an accurate comparison of the resonance energies.) A representative subset [5-7] is shown in Fig. 5 along with the presently available data on $\text{Bi}_2\text{Sr}_2\text{CaCu}_2\text{O}_{8+\delta}$. While we did not confirm the linear relationship between E_{res} and the doping level predicted by the pp model of the resonance peak [20], Fig. 5 suggests that the parameter controlling E_{res} is actually the transition temperature T_c , with $E_{\text{res}}/k_B T_c \sim 5.4$. Since at least in the underdoped regime the super-

conducting gap does not scale with T_c , this observation is not naturally understood within the ph scenario either. Along with some aspects of the sharp “quasiparticle peak” observed in photoemission data in the superconducting state [24], the neutron resonance thus appears to be one of very few spectral features of the superconducting cuprates that scale with T_c . While this may indicate a smooth crossover between a magnon-like collective mode below the ph continuum in the underdoped regime and a simple ph pair production scenario in the overdoped regime, a quantitative theory of such a crossover has thus far not been reported.

Our result supports the conclusion of a neutron scattering study [23] of 3%-Ni substituted $\text{YBa}_2\text{Cu}_3\text{O}_7$ ($T_c=80$ K). Ni substitution is known to reduce T_c but does not affect the hole content. In $\text{YBa}_2(\text{Cu}_{0.97}\text{Ni}_{0.03})_3\text{O}_7$, E_{res} is shifted from 40 meV to ~ 35 meV so that the ratio E_{res}/T_c is preserved, as observed here for overdoped $\text{Bi}_2\text{Sr}_2\text{CaCu}_2\text{O}_{8+\delta}$.

In conclusion, we have shown that the energy of the magnetic resonant mode scales with the superconducting transition temperature in both the underdoped and the overdoped regimes. This result is important for current theoretical efforts [9–13] to develop a unified phenomenology of magnetic and charge spectroscopies of the cuprates.

We gratefully acknowledge discussions with P.W. Anderson, S. Chakravarty, A. Chubukov, E. Demler, W. Hanke, D. Morr, F. Onufrieva, P. Pfeuty, D. Pines, S. Sachdev, and S.C. Zhang. The work at Princeton University was supported by the National Science Foundation under DMR-9809483.

[1] J. Rossat-Mignod *et al.*, *Physica C* **185-189**, 86 (1991).
[2] H.A. Mook *et al.*, *Phys. Rev. Lett.* **70**, 3490 (1993).
[3] H.F. Fong *et al.*, *Phys. Rev. Lett.* **75**, 316 (1995); *Phys. Rev. B* **54**, 6708 (1996).
[4] P. Bourges *et al.*, *Phys. Rev. B* **53**, 876 (1996).
[5] P. Bourges, in *The Gap Symmetry and Fluctuations in High Temperature Superconductors*, edited by J. Bok, G. Deutscher, D. Pavuna and S.A. Wolf. (Plenum Press, 1998) 349.
[6] H.F. Fong *et al.*, *Phys. Rev. B* **61**, 14773 (2000), and references therein.
[7] P. Dai *et al.*, *Science* **284**, 1344 (1999).
[8] H.F. Fong *et al.*, *Nature* **398**, 588 (1999).
[9] Z.X. Shen and J.R. Schrieffer, *Phys. Rev. Lett.* **78**, 1771 (1997).
[10] J.C. Campuzano *et al.*, *Phys. Rev. Lett.* **83**, 3709 (1999); M.R. Norman and H. Ding, *Phys. Rev. B* **57**, R11089 (1998).
[11] A. Abanov and A.V. Chubukov, *Phys. Rev. Lett.* **83**, 1652 (1999).

[12] D. Munzar, C. Bernhard, and M. Cardona, *Physica C* **318**, 547 (1999).
[13] J.P. Carbotte, E. Schachinger, and D.N. Basov, *Nature* **401**, 354 (1999).
[14] D.J. Scalapino and S.R. White, *Phys. Rev. B* **58**, 8222 (1998).
[15] E. Demler and S.C. Zhang, *Nature* **396**, 733 (1998).
[16] S. Chakravarty and H.K. Kee, *Phys. Rev. B* **61**, 14821 (2000).
[17] See, *e.g.*, L. Yin, S. Chakravarty and P.W. Anderson, *Phys. Rev. Lett.* **78**, 3559 (1997); A.A. Abrikosov, *Phys. Rev. B* **57**, 8656 (1998).
[18] See, *e.g.*, I.I. Mazin and V.M. Yakovenko, *Phys. Rev. Lett.* **75**, 4134 (1995); F. Onufrieva, *Physica C* **251**, 348 (1995); D.L. Liu, Y. Zha and K. Levin, *Phys. Rev. Lett.* **75**, 4130 (1995); N. Bulut and D.J. Scalapino, *Phys. Rev. B* **53**, 5149 (1996); A.J. Millis and H. Monien, *Phys. Rev. B* **54**, 16172 (1996); J. Brinckmann and P.A. Lee, *Phys. Rev. Lett.* **82**, 2915 (1999); F. Onufrieva and P. Pfeuty, *cond-mat/9903097*.
[19] A.V. Chubukov, S. Sachdev, and J. Ye, *Phys. Rev. B* **49**, 11919 (1994); D.K. Morr and D. Pines, *Phys. Rev. Lett.* **81**, 1086 (1998); S. Sachdev, C. Buragohain, and M. Vojta, *Science* **286**, 2479 (1999).
[20] E. Demler and S.C. Zhang, *Phys. Rev. Lett.* **75**, 4126 (1995); E. Demler, H. Kohno, and S.C. Zhang, *Phys. Rev. B* **58**, 5719 (1998).
[21] G.D. Gu, K. Takamuku, N. Koshizuka, and S. Tanaka, *J. Crystal Growth* **130**, 325 (1998).
[22] S.H. Han *et al.*, *Physica C* **246**, 22 (1995).
[23] Y. Sidis *et al.*, *Phys. Rev. Lett.* **84**, 5900 (2000).
[24] D.L. Feng *et al.*, *Science* **289**, 277 (2000).

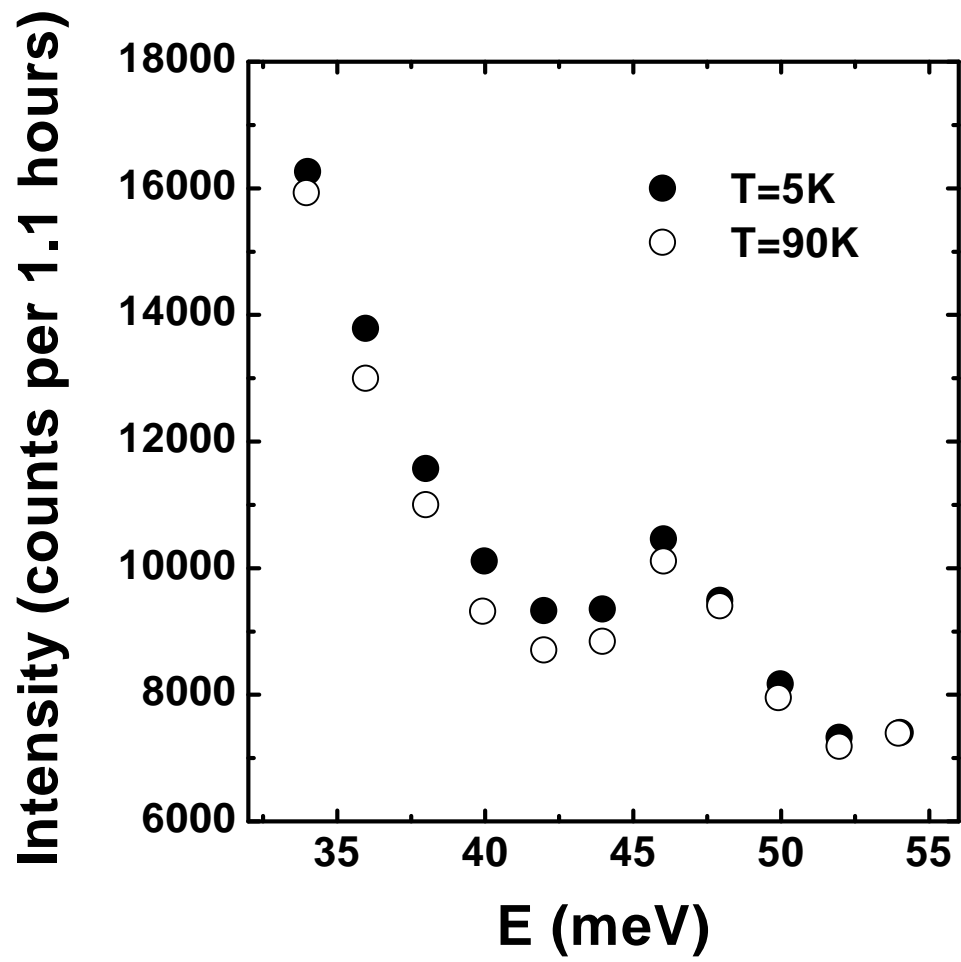
FIG. 1. Raw (unsubtracted) spectra at wave vector $\mathbf{Q} = (0.5, 0.5, -13.2)$ and temperatures 10K and 100K. The large background is mostly due to a multitude of unresolved phonons (see text). The error bars are smaller than the symbol size.

FIG. 2. Closed symbols: Difference spectrum of the neutron intensities at $T = 5$ K ($< T_c$) and $T = 90$ K ($> T_c$), at wave vector $\mathbf{Q} = (0.5, 0.5, -13.2)$ for overdoped $\text{Bi}_2\text{Sr}_2\text{CaCu}_2\text{O}_{8+\delta}$. Open symbols: Data taken under identical conditions in optimally doped $\text{Bi}_2\text{Sr}_2\text{CaCu}_2\text{O}_{8+\delta}$ (Ref. [8]). The bar represents the instrumental energy resolution, The solid lines are the results of fits as described in the text. The dashed line is the resonance energy extracted from fitting the data on optimally doped $\text{Bi}_2\text{Sr}_2\text{CaCu}_2\text{O}_{8+\delta}$.

FIG. 3. Difference spectrum of the neutron intensities at $T = 5$ K ($< T_c$) and $T = 90$ K ($> T_c$), at energy 38 meV. The bar represents the instrumental momentum resolution, the line is a guide-to-the-eye.

FIG. 4. Temperature dependence of the neutron intensity at energy 38 meV and wave vector $\mathbf{Q} = (0.5, 0.5, -13.2)$. The intensity falls to background level above $T_c = 83$ K. The line is a guide-to-the-eye. The insert shows a measurement of the uniform magnetization of a sample from the same batch in an applied field of 10G.

FIG. 5. A synopsis of the resonance peak energy E_{res} in underdoped and optimally doped $\text{YBa}_2\text{Cu}_3\text{O}_{6+x}$ (open symbols, with squares from Ref. [5], circles from Ref. [6], and diamonds from Ref. [7]) and optimally doped and overdoped $\text{Bi}_2\text{Sr}_2\text{CaCu}_2\text{O}_{8+\delta}$ (closed symbols, from Ref. [8] and present work), plotted as a function of the superconducting transition temperature T_c . The shaded areas indicate measures of (or upper bounds on) the intrinsic width of the peak. The error bar on the peak position is of the order of the symbol size.



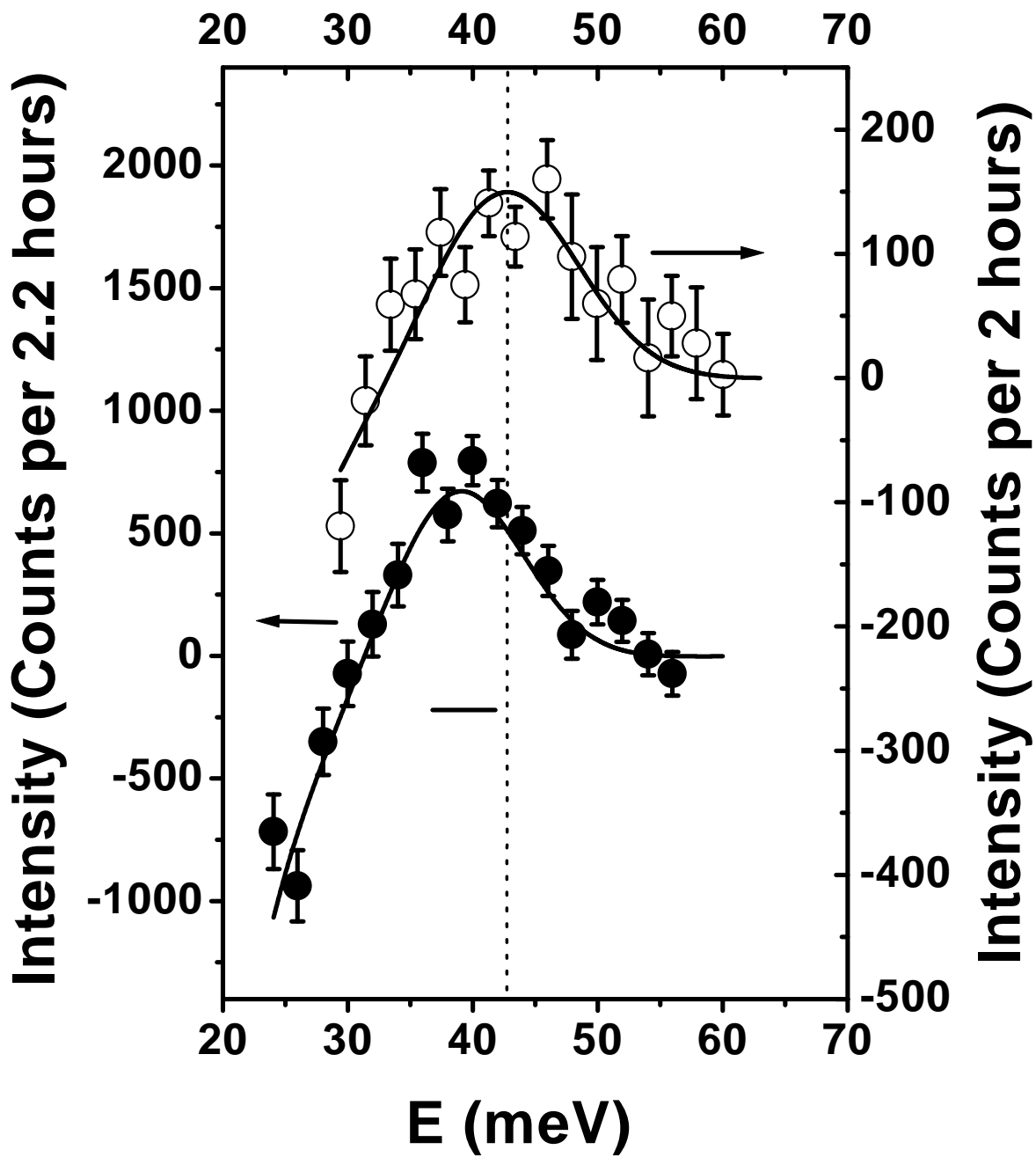


Fig. 3 He et. al.

